

## Supporting Information

# Proximity-Drive Bioorthogonal Reactions via DNA Circuits the Accurate Aptasensing of Non-Nucleic Acid Targets

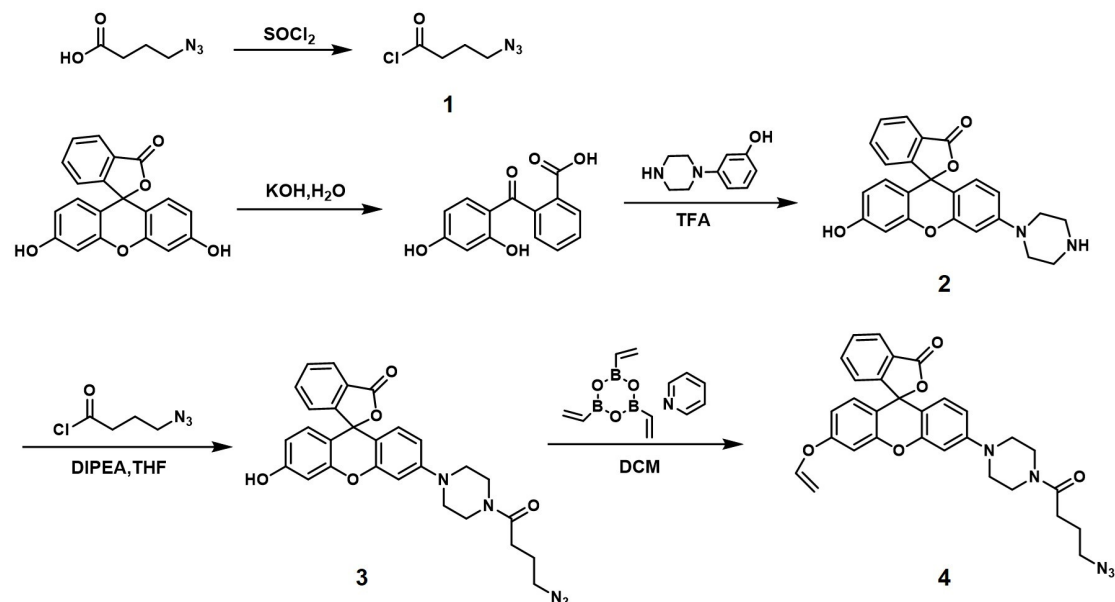
Su-Jing Zhao, Haiyu Guo, Zhenkun Wu,\* and Jian-Hui Jiang

### Table of Contents

S-1	Table of Contents.
S-2	Experimental section.
S-7	Table S1. The sequences used in the study.
S-8	Fig. S1. <sup>1</sup> HNMR spectrum of Tz.
S-9	Fig. S2. <sup>1</sup> HNMR spectrum of PF.
S-10	Fig. S3. Fluorescence and UV spectra of PF and Tz.
S-11	Fig. S4. HPLC analysis and Mass spectra of PF and Tz.
S-12	Fig. S5. HPLC analysis of HA-1 modifications.
S-13	Fig. S6. HPLC analysis of HA-2 modifications.
S-14	Fig. S7. TOF-MS assay of HA-Tz and HA-PF.
S-15	Fig. S8. Structure optimization of AptA-I.
S-16	Fig. S9. Optimization of molar ratio of AptA-I2 to HA-Tz/HA-PF.
S-17	Fig. S10. Linear region of fluorescence intensities versus ATP concentrations.
S-18	Fig. S11. Fluorescence spectra of PBRC probes with ATP and other analogue molecules.
S-19	Fig. S12. Selectivity assay of PBRC probes.
S-20	Fig. S13. Real-time fluorescence responses of PBRC probes in diluted FBS solution.
S-21	Fig. S14. Real-time imaging of MCF-7 cells incubated with PBRC probes.
S-22	Fig. S15. Optical sectioning imaging of MCF-7 cells along with Z-axis.
S-23	Fig. S16 Measurement of intracellular ATP concentrations in MCF-7 cells with different treatments.
S-24	Fig. S17. Evaluation of ATP expression levels in different cell lines.
S-25	Fig. S18. HPLC analysis of Ht-1 and Ht-2 conjugation.
S-26	Fig. S19. TOF-MS of Ht-Tz and Ht-PF.
S-27	Fig. S20. Structure optimization of AptT-I.
S-28	Fig. S21. Thrombin detection using PBRC probes.

**Reagents and Materials.** 4-azidobutyric acid, thionyl chloride, fluorescein, 1-(3-hydroxyphenyl) piperazine, vinyl boronicanhydride pyridine complex, nickel (II) trifluoromethanesulfonate, 3-cyanobenzyl alcohol, phosphorus tribromide, sodium azide, acetic acid, triethylamine and dimethyl sulfoxide were purchased from Energy Chemical (Shanghai, China). All oligonucleotides were synthesized and purified by Sangon Biotech Co. Ltd., (Shanghai, China). The sequences were shown in Table S1. ATP, UTP, CTP, GTP, Oligomycin, and Thrombin was obtained from Sigma-Aldrich (St. Louis, USA). Bovine Serum Albumin (BSA) and Trypsin were purchased from Genview (USA). Recombinant ALKBH2, ALKBH3 and FTO were bought from Active Motif (Carlsbad, USA). Cell lines HEK 293T, HeLa and MCF-7 were obtained from Cell Bank of the Committee on TyPe Ctture Collection of the Chinese Academy of Sciences (Shanghai, China). DMEM cell culture medium, penicillin-streptomycin were obtained from Thermo Scientific HyClone (MA, USA). Lipofectamine 3000 and Opti-MEM were purchased from Invitrogen (MA, USA). The ATP assay kit was purchased from Beyotime Biotechnology (China). All reagents were analytical grade and used without further purification. All solutions were prepared using ultrapure water that was obtained through a Millipore Milli-Q water purification system (Billerica, MA, USA) with an electrical resistance >18.25 MΩ.

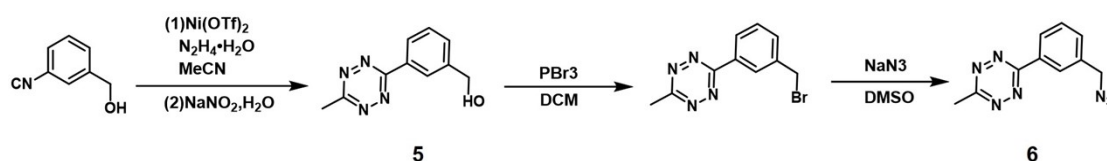
### Synthesis of Pre-fluorophore (PF)



A vinyl ether caged fluorophore was synthesized according to previous procedures.<sup>1</sup> In brief, (a) thionyl chloride (1.2 equiv) was added into 4-azidobutyric (1 equiv) at 0 °C. The reaction was left at room temperature for 15 h and then was left for another 1 h at 40 °C. The resulting mixture was condensed to afford compound 1 for further used. (b) Fluorescein (1 equiv) and  $\text{KOH}$  (20 equiv) was refluxed in  $\text{H}_2\text{O}$  for 5 h (35 ml). After the reaction was

completed, it was cooled to 0 °C and acidified with hydrochloric acid, followed by extracted with EtOAc. The concentrated extract was crystallized in DCM to afford 2-(2,4-dihydroxybenzoyl) benzoic acid. Next, the prepared chemical 2-(2,4-dihydroxybenzoyl) benzoic acid (1 equiv) and 1-(3-hydroxyphenyl)-piperazine (1 equiv) were refluxed in TFA at 95 °C for 3 h, the resulting mixture was precipitated in EtOAc and redissolved in MeOH, then evaporated under reduced pressure to give a red solid product. The red solid product was purified by silica column chromatography using MeOH-CH<sub>2</sub>Cl<sub>2</sub> 1:1 (v/v) to afford compound 2. (c) Compound 1 (1 equiv) in DCM and N,N-diisopropylethylamine (1.1 equiv) in THF were dropwise added into compound 2. The reaction was kept stirring at 25 °C for 2 h. The resulting mixture was condensed and purified by silica column chromatography using MeOH-CH<sub>2</sub>Cl<sub>2</sub> 1:10 (v/v) to yield compound 3 as a red solid. (d) Copper (II) acetate (1 equiv) in anhydrous DCM (10 mL) was stirred at 25 °C for 10min. Compound 3 (1 equiv), vinyl boroncanhydride pyridine complex (1 equiv) and pyridine (10 equiv) were then added. The mixture was stirred at room temperature for 50 h and extracted with EtOAc. The organic layers were washed with 2 M HCl, dried over magnesium sulfate, and concentrated in vacuo. The crude product was purified by silica column chromatography using MeOH-CH<sub>2</sub>Cl<sub>2</sub> 1:10 (v/v) to afford the final product of pre-fluorophore (compound 4) and characterized by H-Nuclear Magnetic Resonance spectroscopy (HNMR). <sup>1</sup>HNMR (400 MHz, CDCl<sub>3</sub>) δ (ppm): 8.04 (1H, d, J = 7.2 Hz, Ar-H), 7.62-7.71 (2H, m, Ar-H), 7.17 (1H, d, J = 7.6 Hz, Ar-H), 6.89 (1H, d, J = 6.4 Hz, CH=), 6.61-6.78 (6H, m, Ar-H), 4.87-4.91 (1H, dd, J<sub>1</sub> = 14.8 Hz, J<sub>2</sub> = 2.0 Hz, CH=), 4.56-4.57 (1H, dd, J<sub>1</sub> = 6.0 Hz, J<sub>2</sub> = 1.6 Hz, CH=), 3.79 (2H, t, J = 5.2 Hz, CH<sub>2</sub>), 3.65 (2H, t, J = 5.2 Hz, CH<sub>2</sub>), 3.43 (2H, t, J = 6.4 Hz, CH<sub>2</sub>), 3.27 (4H, t, J = 5.6 Hz, 2 × CH<sub>2</sub>), 2.48 (2H, t, J = 6.8 Hz, CH<sub>2</sub>), 1.95-2.01 (2H, m, CH<sub>2</sub>).

### Synthesis of tetrazine (Tz)



Tetrazine molecules was synthesized according to previous procedures.<sup>1</sup> In brief, (a) 3-cyanobenzyl alcohol (1 equiv), Nickel (II) trifluoromethanesulfonate (0.2 equiv), and hydrazine monohydrate (11 mL) in acetonitrile were refluxed at a nitrogen-filled flask at 60 °C for 20 h. Then the reaction mixture was cooled to 25 °C, followed by adding sodium nitrite solution (5 equiv). After that, 1M HCl solution was slowly added to adjust pH value to 3. The mixture was extracted with DCM and purified using CH<sub>2</sub>Cl<sub>2</sub>-EtOAc 2:1 (v/v) as the eluent to give

compound 5. (b) Phosphorous tribromide (3 equiv) was dropwise added to compound 5 (6.1 equiv) at 0 °C in DCM. After the reaction was kept at room temperature for another 2.5 h, the mixture was quenched with water and extracted with DCM, the organic layer was then washed with brine, concentrated in vacuo. The crude product (1 equiv) from the previous step and sodium azide (7 equiv) were heated in DMSO at 85 °C overnight. After that, the reaction was quenched with H<sub>2</sub>O and the product was extracted with EtOAc. The organic layer was washed with brine (20 ml), dried over magnesium sulfate, concentrated in vacuo to yield tetrazine (compound 6) as a purplish red solid and characterized by H-Nuclear Magnetic Resonance spectroscopy (HNMR). <sup>1</sup>HNMR (400 MHz, CDCl<sub>3</sub>) δ (ppm): 8.61 (2H, d, J = 8.4 Hz, Ar-H), 7.59-7.69 (2H, m, Ar-H), 4.54 (2H, s, CH<sub>2</sub>), 3.15 (3H, s, CH<sub>3</sub>).

### **Characterization of the reaction between PF and Tz.**

The synthesized PF and Tz were firstly dissolved in DMSO at the final concentration of 10 mM and 20 mM, respectively.

For fluorescence assay, the solution of PF (50 μM) and Tz (5 mM) was reacted in DMSO at 60 °C for 5 h. Fluorescence spectra was then collected at room temperature in a 20 μL quartz cuvette using a FS5 spectrometer. The excitation wavelength was 510 nm, and the emission was measured from 520 to 700 nm.

For HPLC assay, PF (100 μM) and Tz (10 mM) were incubated in DMSO at 60 °C for 5 h. The sample was lyophilized to remove the solvent, and then redissolved in MeOH. The product was finally analyzed using an Agilent 1260 HPLC system equipped with a C18 column (150 × 3.0 mm, 5 μm). The separation system was run with a prepared solution (H<sub>2</sub>O: MeOH = 25: 75, v: v. 0.05% Trifluoroacetate was contained in H<sub>2</sub>O). Flow rate: 0.5 mL/min; detection wavelength: 510 nm.

### **Oligonucleotides conjugation.**

DBCO-modified DNA hairpins, HA-1 and HA-2 were firstly dissolved in 200 μL ddH<sub>2</sub>O to a final concentration of 20 μM, respectively. A solution of Tz (20 mM) and PF (20 mM) in DMSO (200 μL) were then added in the solution of HA-1 and HA-2, respectively. The mixture was left at room temperature for 6 h and reaction products were analyzed by HPLC.

### **Purification of modified oligonucleotides.**

HA-Tz and HA-PF DNA products were purified using an Agilent 1260 HPLC system equipped with a C18 column (150 × 3.0 mm, 5 μm). The separation system used 0.1 M TEAA (Triethylamine: acetic acid = 1: 1, c: c) as mobile phase A and MeCN as mobile phase B. The elution procedure is as follows: Initial conditions 95% A, 5% B, hold 5 min then a linear gradient starting at 5 min and ending at 25 min with 55% A, 45% B; Finally, another linear gradient

starting at 25 min and ending at 80 min with 5% A, 95% B. flow rate: 1 mL min<sup>-1</sup>; detection wavelength: 260 nm. Collect purified modified oligonucleotides and lyophilized to remove solvent. The purity and concentration of HA-Tz and HA-PF were verified by TOF-MS and Nanodrop 2000 UV-vis spectrophotometer.

#### **Gel electrophoresis analysis.**

All the samples were performed in 10  $\mu$ L 50 mM Tris-MgCl<sub>2</sub> buffer (137 mM NaCl; 12.5 mM MgCl<sub>2</sub>, pH = 7.4) incubating at 37 °C for 6 h. 1  $\mu$ L 10  $\times$  loading buffer was added into each sample for gel electrophoresis experiments. Gel electrophoresis analysis was carried out on 3% (w/w) agarose gels in 0.5  $\times$  TBE buffer at a constant potential of 100 V for 1 h. All gels were imaged and analyzed using Tanon 4200SF gel imaging system (Tanon Science & Technology Co. Ltd., China).

#### **Fluorescence detection in vitro.**

Hairpin of AptA-I2, HA-Tz, HA-PF was diluted to 2  $\mu$ M using Tris-MgCl<sub>2</sub> buffer (50 mM Tris, 137 mM NaCl, 12.5 mM MgCl<sub>2</sub>, pH = 7.4). Then, samples were heated at 95 °C for 5 min, cooled to 0 °C for 5 min and finally left at room temperature for another 2 h to enable the correct folding.

For ATP assay, PRBC probes (40 nM AptA-I2, 200 nM HA-Tz and HA-PF) were incubated with different concentrations of ATP for 6 h at 37 °C. Fluorescence spectrums were then collected using a FS5 Spectrofluorometer. The excitation wavelength was 510 nm, and the emission was measured from 520 to 700 nm.

For thrombin assay, PRBC probes (40 nM AptT-I1, 200 nM HA-Tz and HA-PF) were incubated with different concentrations of thrombin for 6 h at 37 °C. Fluorescence spectrums were then collected using a FS5 Spectrofluorometer. The excitation wavelength was 510 nm, and the emission was measured from 520 to 700 nm.

#### **Confocal imaging.**

HEK 293T, HeLa and MCF-7 cells that were seeded on the confocal dishes were transfected with PRC probes (40 nM AptA-I2, 200 nM HA-Tz, 200 nM HA-PF) using a commercial transfection reagent lipofectamine 3000 in Opti-MEM for 6 h and then taken for confocal imaging directly using a Nikon TI-E SI confocal laser scanning microscope.

For confocal imaging of intracellular ATP with different concentration, MCF-7 cells were pretreated with Ca<sup>2+</sup> (10 mM) or oligomycin (10  $\mu$ M) at 37 °C for 30 min to upregulate or downregulate ATP expression levels, respectively. Then, PBRC probes (40 nM AptA-I2, 200 nM HA-Tz, 200 nM HA-PF) were transfected with cells using lipofectamine 3000 at 37 °C for another 6 h. MCF-7 cells were finally washed with 1x PBS and confocal images were acquired using Nikon TI-E SI confocal laser scanning microscope.

#### **Flow cytometric analysis**

PBRC probes (40 nM AptA-I2, 200 nM HA-Tz and 200 nM HA-PF) were incubated with cells ( $1 \times 10^5$  cells) at 37 °C for 6 h. Then, cells were washed three times with cold 1x PBS and detached using 200  $\mu$ L 0.25% trypsin. After that, cells were centrifuged at 1000 rpm for 3 min followed by washing with 1x PBS and finally resuspended in 400  $\mu$ L PBS for flow cytometric assay using a CytoFLEX™ flow cytometer (Beckman Counter, Inc., USA).

#### Reference

(1) Zhao, S. J.; Zheng, P.; Wu, Z.; Jiang, J. H. DNA-Templated Bioorthogonal Reactions via Catalytic Hairpin Assembly for Precise RNA Imaging in Live Cells. *Anal. Chem.* 2022, 94, 2693-2698.

**Table S1. Sequences of oligonucleotides.**

Name	Sequence (5'-3')
AptA-I0	ACCTGGGGGAGTATTGCGGAGGAAGGTGGTACGTTTATGCACGCACCTTCC
AptA-I1	ACCTGGGGGAGTATTGCGGAGGAAGGTGCTACGTTTATGCACGCACCTTCC
AptA-I2	ACCTGGGGGAGTATTGCGGAGGAAGGTGCTACGTTTATGCACGCACCTTCTC
AptA-I3	ACCTGGGGGAGTATTGCGGAGGAAGGTGCTACGTTTATGCACGCACCTTCTC
mAptA-I2	TGGACCCCGAGTATTGCGGAGGAAGGTGCTACGTTTATGCACGCACCTTCTC
HA-1	GGAAGGTGCGTGCATAAACGTAGCT(DBCO)AAGCATGCTACGTTTATGCACGCA
HA-2	(DBCO)GCTACGTTTATGCACGCACCTTCTGCGTGCATAAACGTAGCATGCTTA
HA-C	GCT(BHQ2)ACGTTTATGCACGCACCTTCTGCGTGCATAAACGT(FAM)AGCATGCTTA
AptT-I0	GGTTGGTGTGGTTGGTCATAGAGCGGCTTAGGATATGACCAAC
AptT-I1	GGTTGGTGTGGTTGGTCATAGAGCGGCTTAGGATATGACCAACC
AptT-I2	GGTTGGTGTGGTTGGTCATAGAGCGGCTTAGGATATGACCAACCA
AptT-I3	GGTTGGTGTGGTTGGTCATAGAGCGGCTTAGGATATGACCAACCAC
Ht-1	GGCTTAGGATATGACCAAATTGCT(DBCO)ATTGGTCATATCCTAAGCCGCTCTA
Ht-2	(DBCO)TAGCAATTTGGTCATATCCTAAGCCTAGAGCGGCTTAGGATATGACCAA

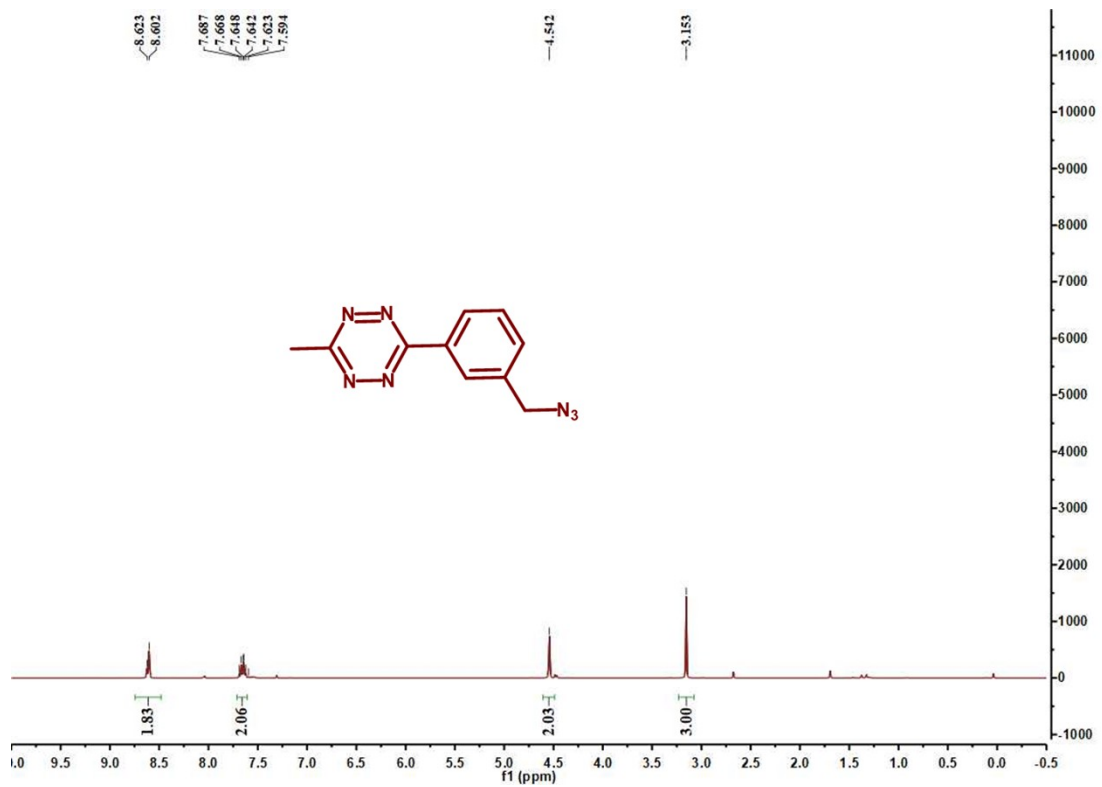


**Fig. S1** <sup>1</sup>H NMR spectrum of Tz in CDCl<sub>3</sub>.



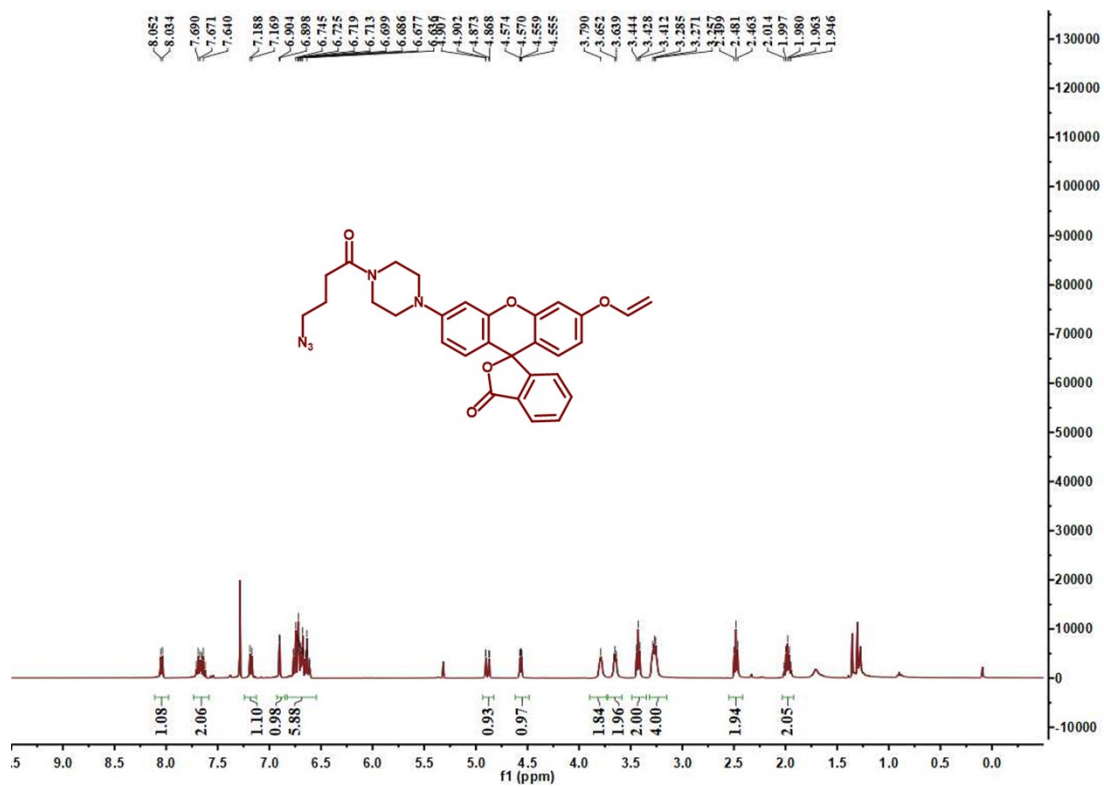
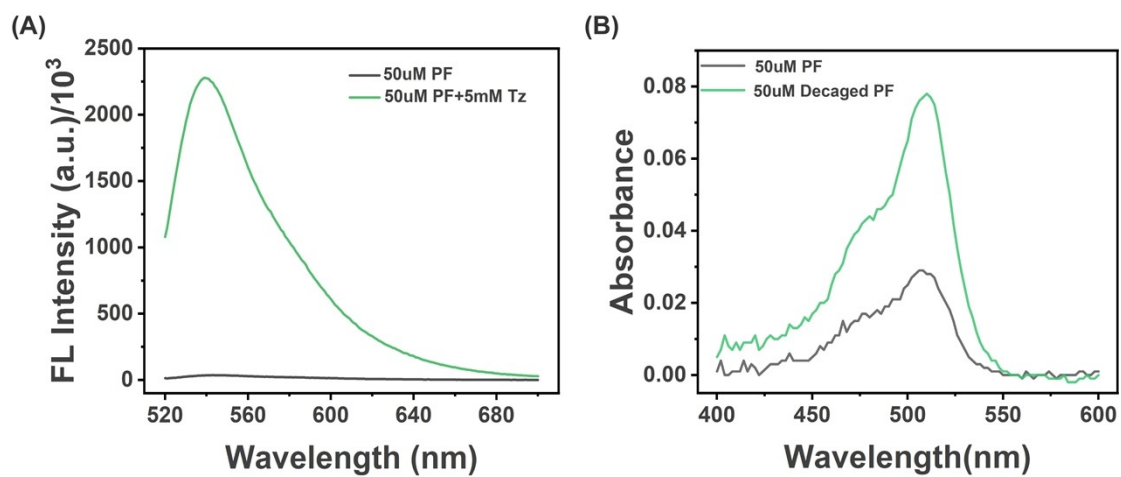
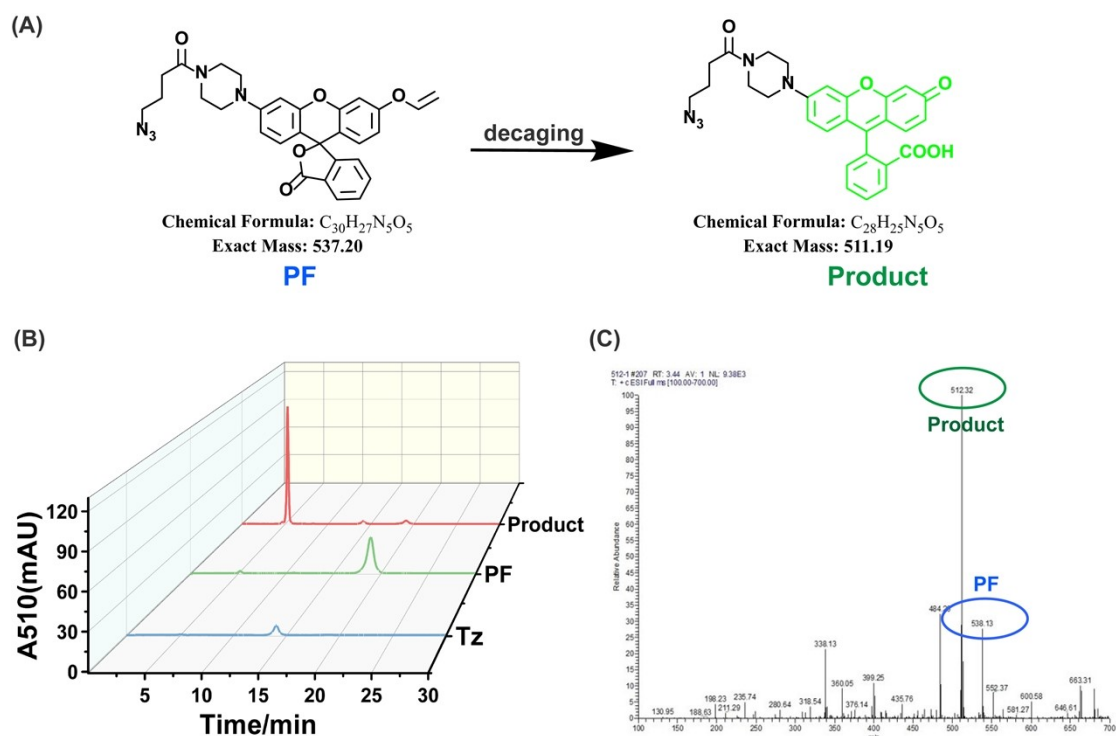


Fig. S2  $^1\text{H}$ NMR spectrum of PF in  $\text{CDCl}_3$ .



**Fig. S3** Characterization of the bioorthogonal reaction between PF and Tz. (A) Fluorescence spectra of PF and degraded product. (B) UV-Vis absorption spectra of PF and degraded product.



**Fig. S4** Reaction mechanism of PF and Tz. (A) Schematic illustration of Tz-mediated decaging reaction. (B) HPLC analysis of PF (100  $\mu$ M, 10  $\mu$ L), Tz (10 mM, 10  $\mu$ L) and the decaged product. (C) Mass spectrometry analysis of the reaction solution of PF and Tz. Exact Mass of PF: 537.20; Found Mass:  $[M+H]^+$  = 538.13; Exact Mass of the decaged product: 511.19; Found Mass:  $[M+H]^+$  = 512.32.

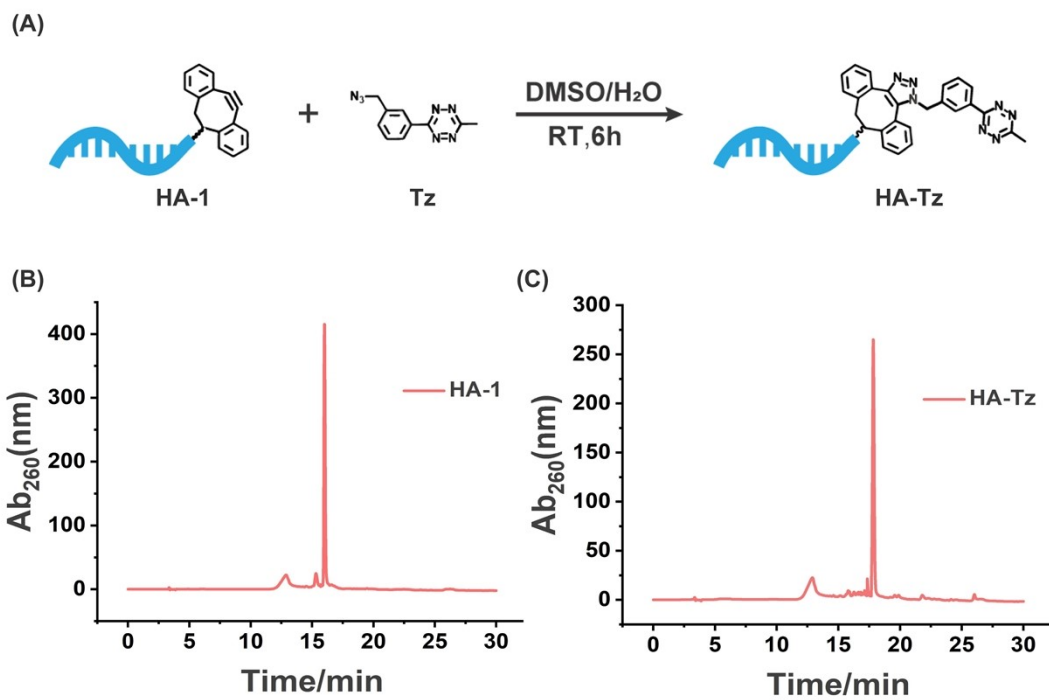


**Fig. S5** HPLC analysis of oligonucleotide modifications. (A) Schematic illustration of HA-1 and Tz conjugation via DBCO and azide reaction. (B) Retention time of HA-1. (C) Retention time of HA-Tz.

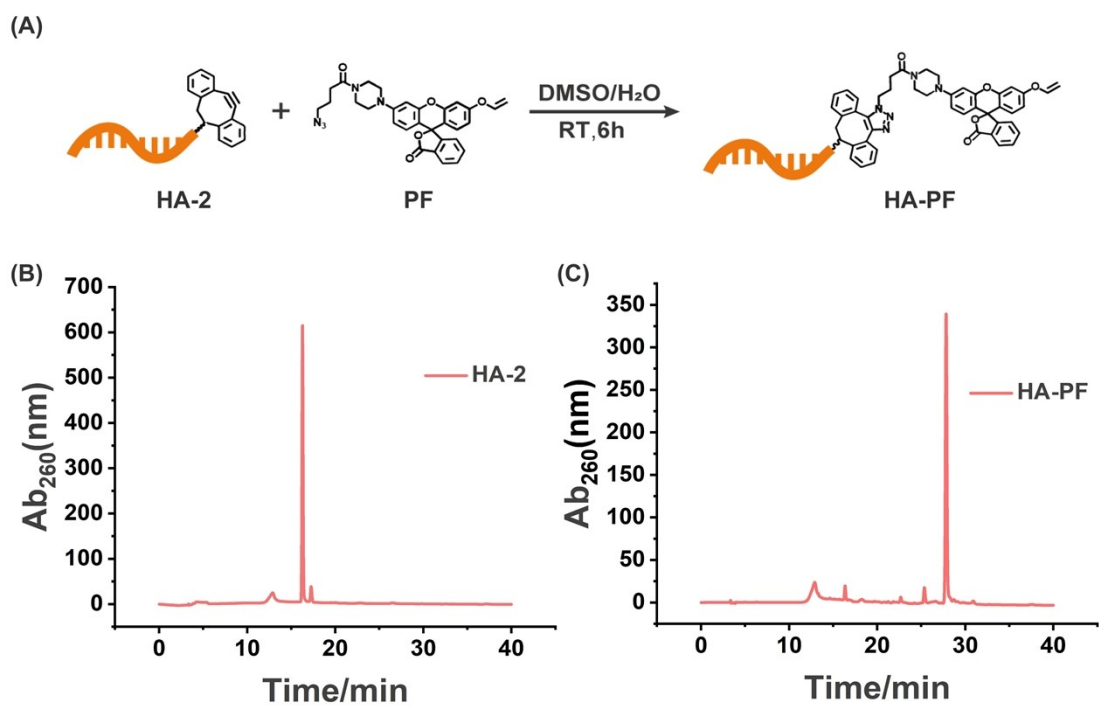


**Fig. S6** HPLC analysis of oligonucleotide modifications. (A) Schematic illustration of HA-2 and PF conjugation via DBCO and azide reaction. (B) Retention time of HA-2. (C) Retention time of HA-PF.

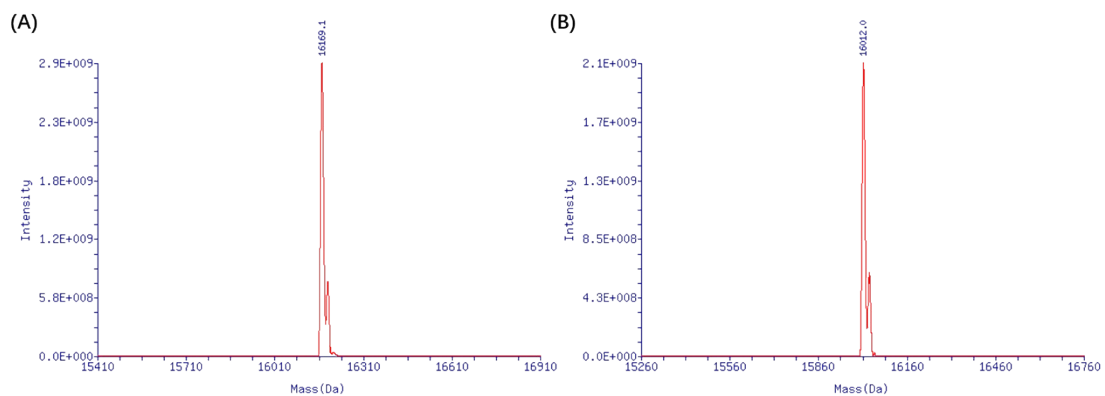


**Fig. S7** TOF-MS analysis of modified oligonucleotides. (A) HA-Tz: Calculated Mass: 16170.7; Theoretical Mass: 16169.1. (B) HA-PF: Calculated Mass: 16014.5; Theoretical Mass: 16012.0.

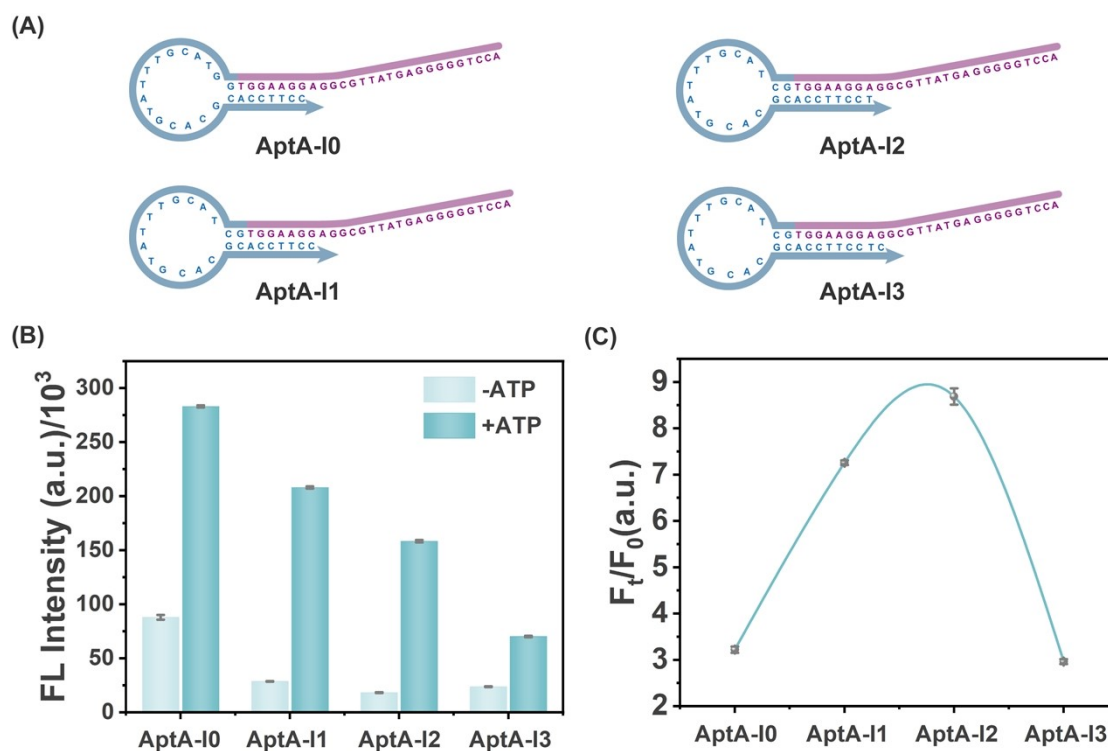


**Fig. S8** Structure optimization of AptA-I. (A) Structure illustration of AptA-I. (B) Histogram of fluorescence intensities of different AptA-I sequences with or without ATP (500  $\mu$ M). (C) Signal ratio  $F_t/F_0$  ( $F_t$ : PBRC probes with 500  $\mu$ M ATP;  $F_0$ : PBRC probes without ATP). Error bars represent three independent experiments.

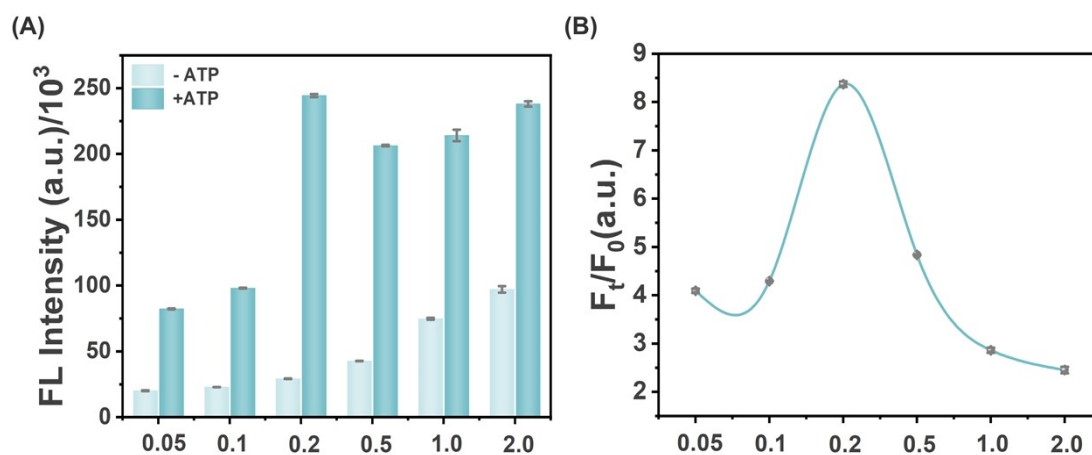


**Fig. S9** Optimization of molar ratio of AptA-I2 to HA-Tz/HA-PF. (A) Histogram of fluorescence intensities of PBRC probes with different ratio in presence or absence of ATP (500  $\mu$ M). (B) Signal ratio  $F_t/F_0$  ( $F_t$ : PBRC probes with 500  $\mu$ M ATP;  $F_0$ : PBRC probes without ATP) at different ratio values. Error bars represent three independent experiments.



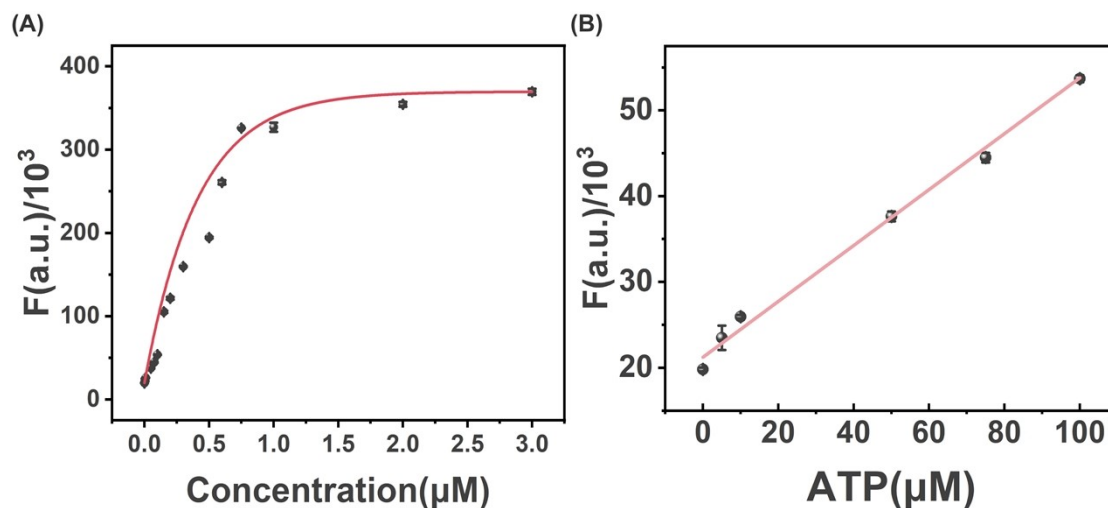


**Fig. S10** (A) Dynamic fluorescence responses of PBRC probes with between different ATP concentrations. (B) Linear region of fluorescence intensities versus ATP concentrations. Error bars represent three independent experiments.

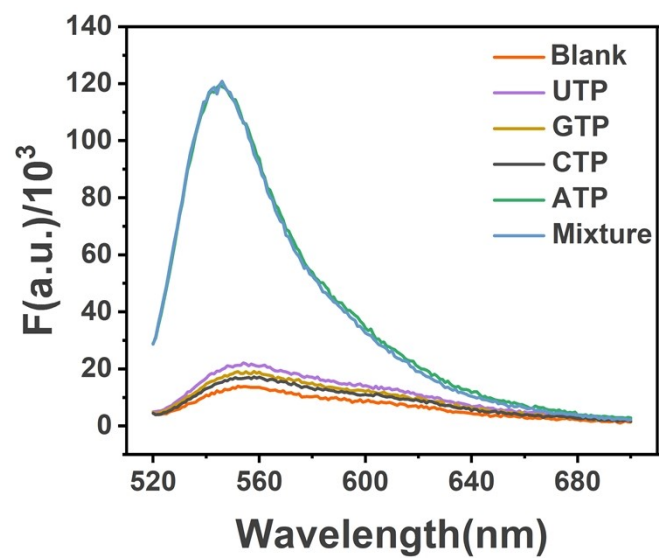


**Fig. S11** Fluorescence spectra of PBRC probes with ATP (500  $\mu\text{M}$ ) and other analogue molecules (500  $\mu\text{M}$ ).

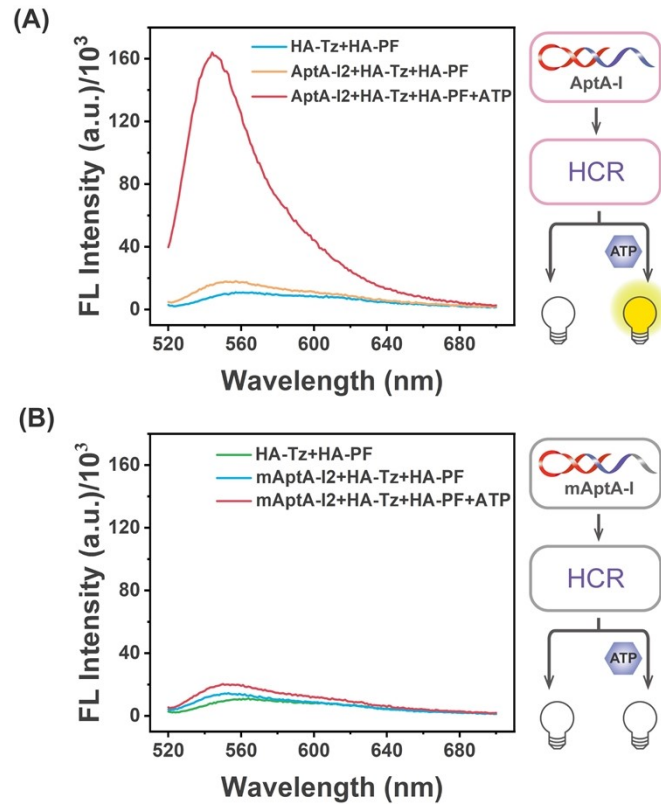


**Fig. S12** Selectivity assay of PBRC probes. (A) Fluorescence response of PBRC probes containing 40 nM AptA-I2, 200 nM HA-Tz, and 200 nM HA-PF. (B) Fluorescence responses of control PBRC probes containing 40 nM mAptA-I2, 200 nM HA-Tz, and 200 nM HA-PF.

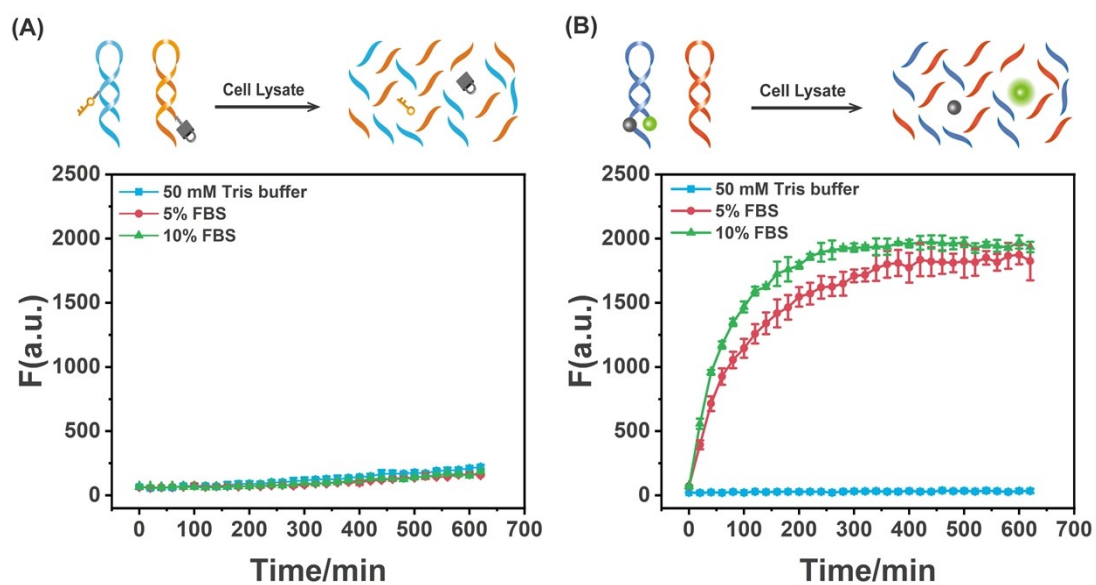


**Fig. S13** Real-time fluorescence responses of PBRC probes and control HCR circuits with classical fluorophore and quencher design in Tris buffer or diluted FBS solution. (A) 200 nM HA-Tz and 200 nM HA-PF were incubated in 20  $\mu$ L 50 mM Tris buffer containing 0  $\mu$ L, 1  $\mu$ L and 2  $\mu$ L FBS at 37  $^{\circ}$ C, respectively. (B) 200 nM HA-1, and 200 nM HA-C with FAM and BHQ1 were incubated in 20  $\mu$ L 50 mM Tris buffer containing 0  $\mu$ L, 1  $\mu$ L and 2  $\mu$ L FBS at 37  $^{\circ}$ C, respectively.

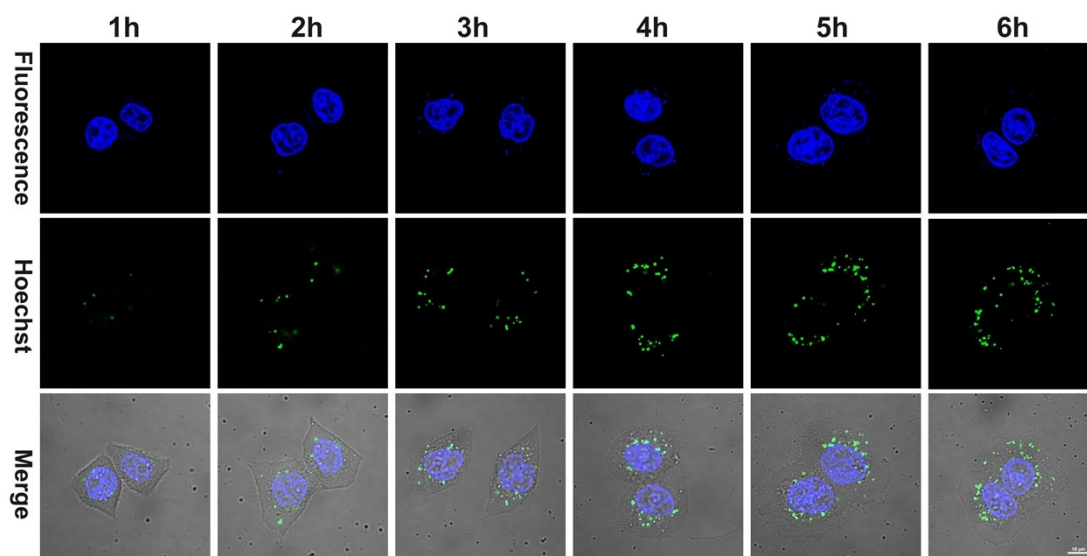


**Fig. S14** Real-time imaging of MCF-7 cells incubated with 500  $\mu$ L Opti-MEM solution containing 40 nM AptA-I2, 200 nM HA-Tz and 200 nM HA-PF. Scale bar: 10  $\mu$ m.

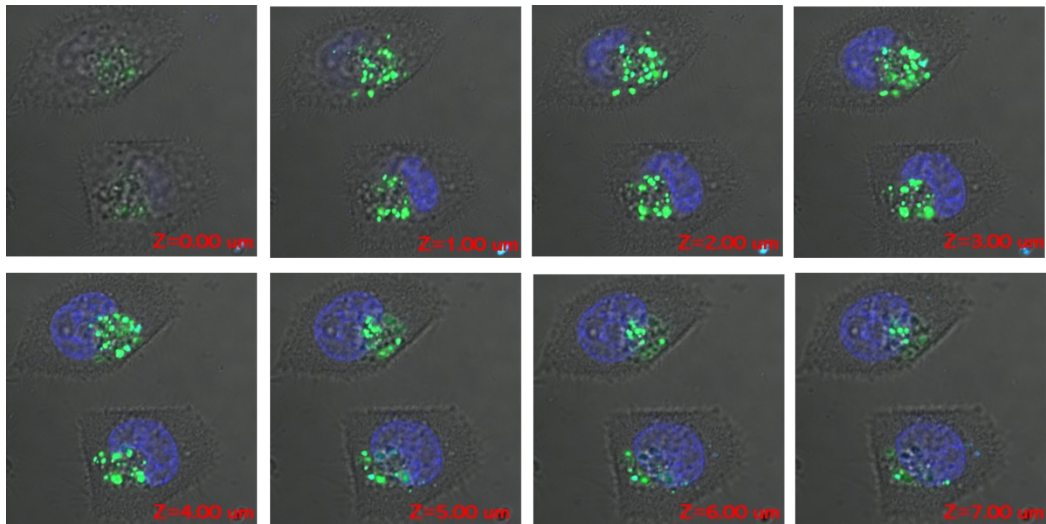


**Fig. S15** Optical sectioning imaging of MCF-7 cells along with Z-axis. MCF-7 cells were incubated with 500  $\mu$ L Opti-MEM solution containing 40 nM AptA-I2, 200 nM HA-Tz and 200 nM HA-PF for 6 h.

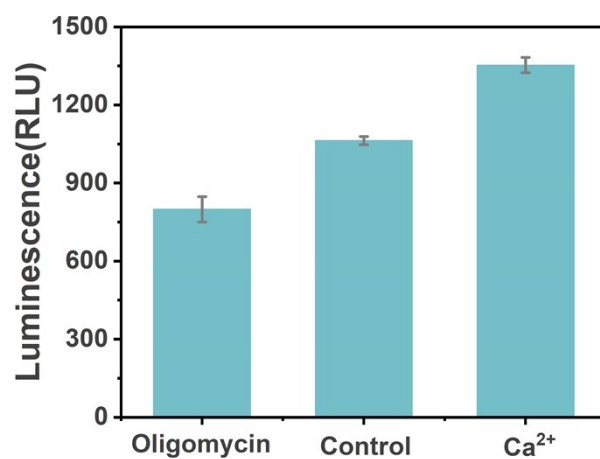


**Fig. S16** Intracellular concentrations of ATP in MCF-7 cells without any treatment or treated with oligomycin and Ca<sup>2+</sup>. The luminescence signals of ATP were obtained using a commercial ATP assay kit based on the luciferin-luciferase bioluminescence method.

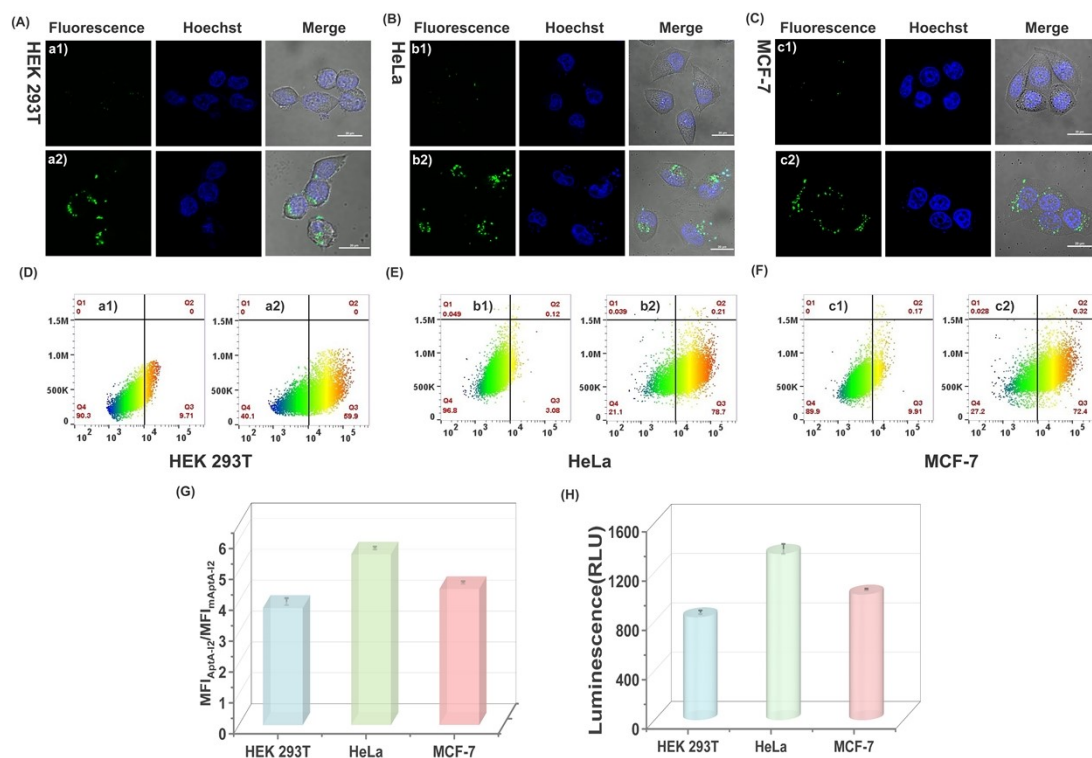


**Fig. S17** Evaluation of ATP expression levels in different cell lines. (A-C) Confocal imaging of HEK 293T, HeLa, and MCF-7 cells transfected with PBRC probes (40 nM AptA-I2, 200 nM HA-Tz, and 200 nM HA-PF) for 6 h, respectively. Scale bar: 20  $\mu$ m. (D-F) Flow cytometric analysis of HEK 293T, HeLa, and MCF-7 cells transfected with control PBRC probes (a1, b1, and c1), or PBRC probes (a2, b2, and c2), respectively. (G) Ratio of mean fluorescence intensities calculated from part (D-F). (H) Intracellular ATP concentrations in HEK 293T, MCF-7 and HeLa using a commercial ATP assay kit. Error bars represent three independent experiments.



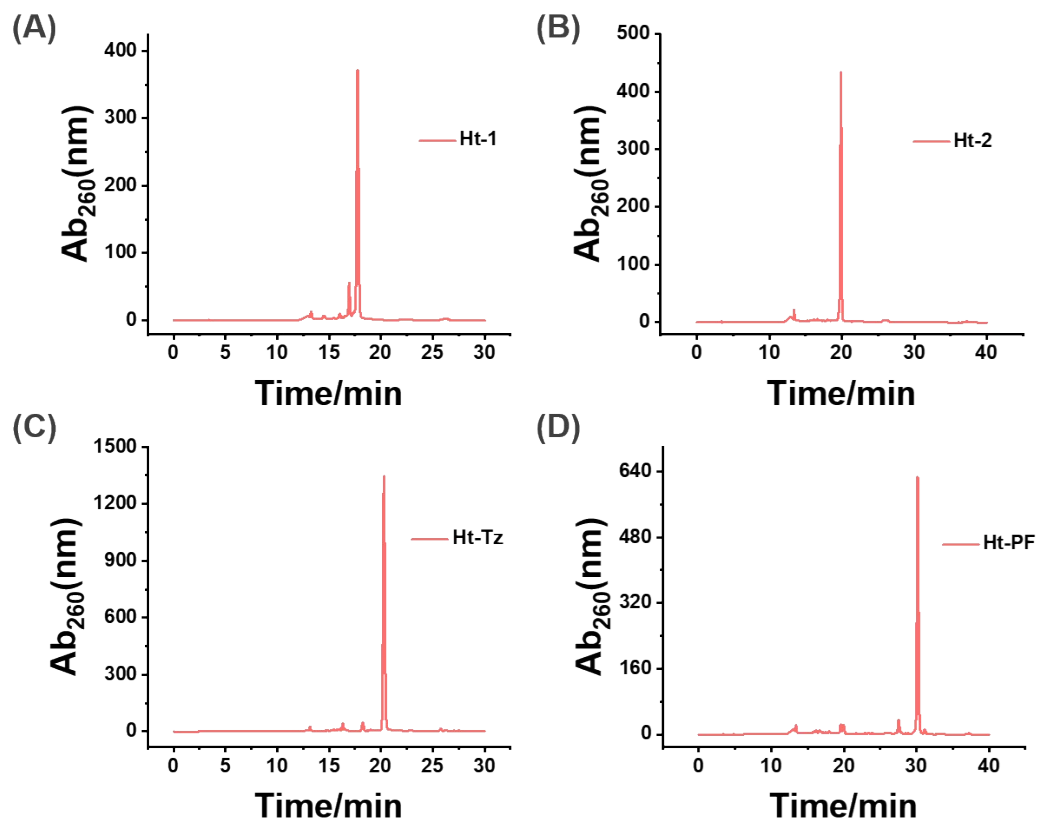


**Fig. S18** HPLC analysis of oligonucleotides conjugation. (A) Retention time of Ht-1. (B) Retention time of Ht-2. (C) Retention time of Ht-Tz. (B) Retention time of Ht-PF.

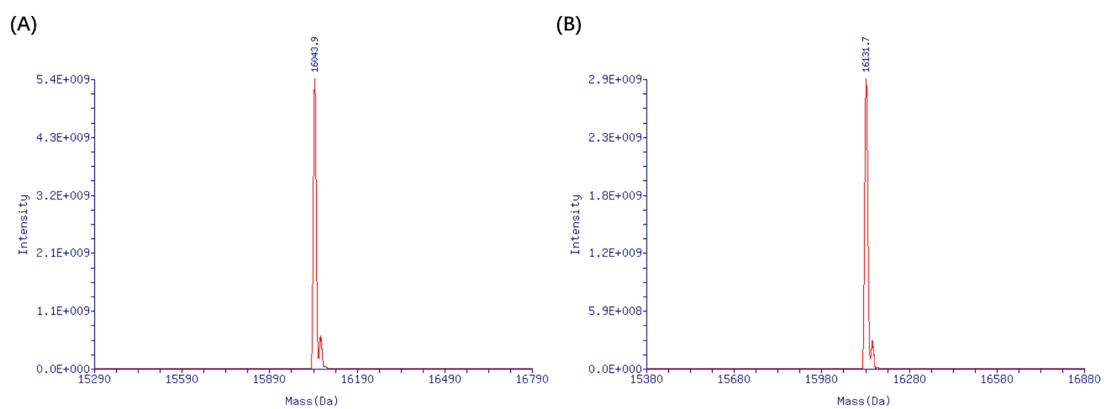


**Fig. S19** TOF-MS of modified oligonucleotides. (A) Ht-Tz: Calculated Mass: 16046.6; Theoretical Mass: 16043.9. (B) Ht-PF: Calculated Mass: 16135.6; Theoretical Mass: 16131.7.

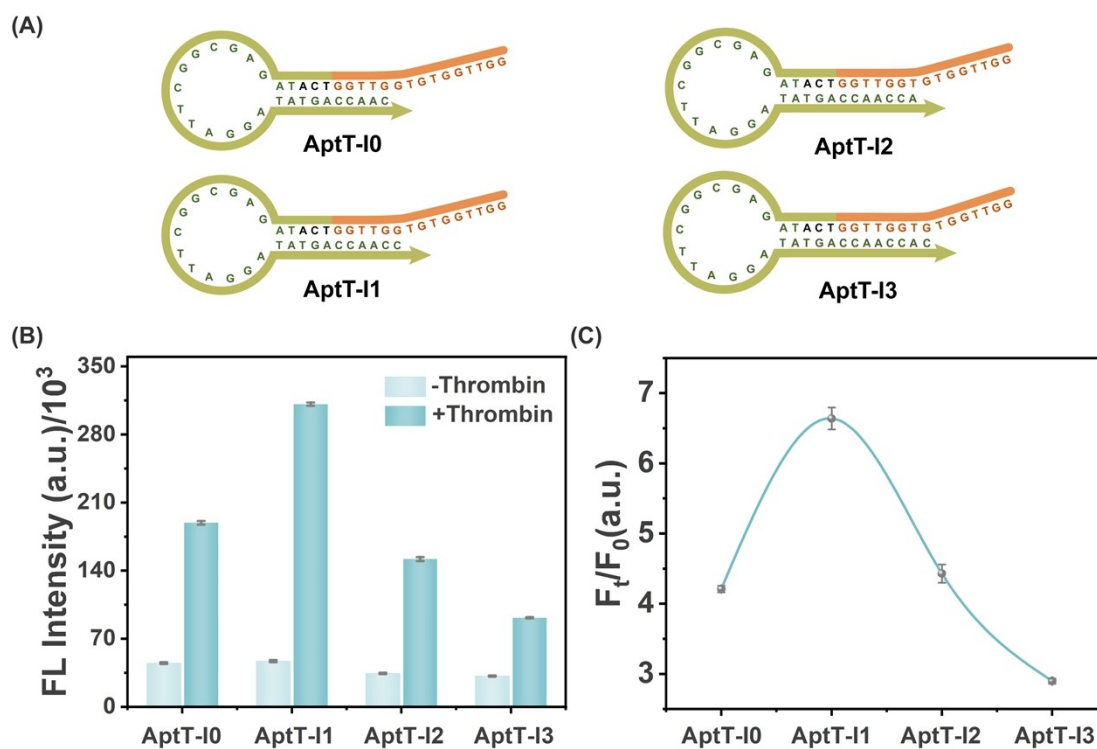


**Fig. S20** Structure optimization of AptT-I. (A) Structure illustration of AptT-I. (B) Histogram of fluorescence intensities of different AptT-I sequences with or without thrombin proteins (500 nM). (C) Signal ratio  $F_t/F_0$  ( $F_t$ : PBRC probes with 500 nM thrombin;  $F_0$ : PBRC probes without thrombin). Error bars represents three independent experiments.

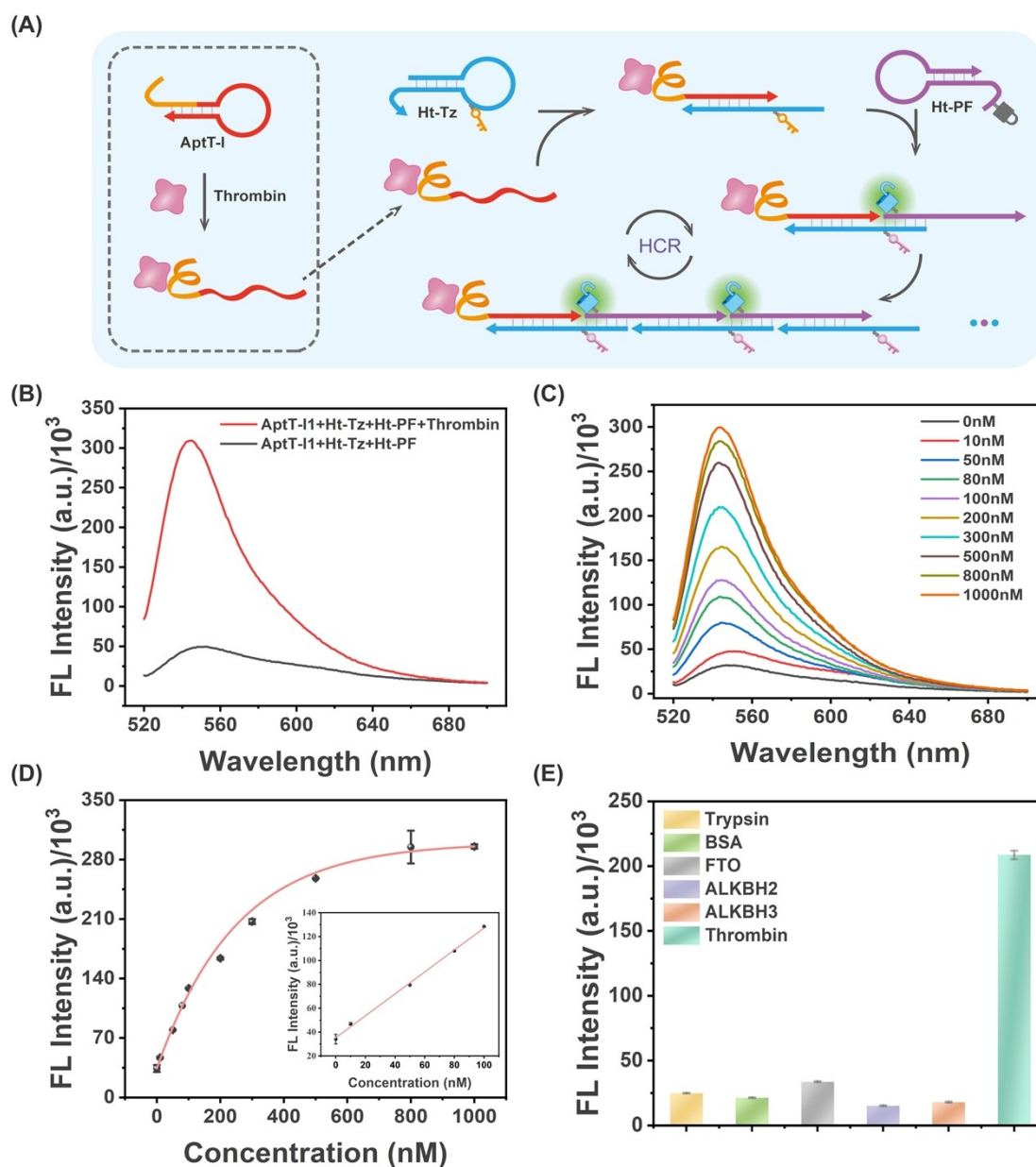


**Fig. S21** Thrombin detection using PBRC probes. (A) Schematic illustration of PBRC probes for aptasensing of thrombin. (B) Feasibility assay of PBRC probes. (C) Sensitivity assay of PBRC probes. (D) Plot of fluorescence intensities at 545 nm versus different thrombin concentrations. The insert Fig. shows the linear detection region. Error bars represent standard deviations from three independent experiments. (E) Selectivity assay of PBRC probes. The concentration of each protein was 500 nM. Error bars represent standard deviations from three independent experiments.